# Smek1/2 is a nuclear chaperone and cofactor for cleaved Wnt receptor Ryk, regulating cortical neurogenesis

Wen-Hsuan Chang[a,b,1], Si Ho Choi[a,c,1,2], Byoung-San Moon[a], Mingyang Cai[a], Jungmook Lyu[a,d], Jinlun Bai[a], Fan Gao[a], Ibrahim Hajjali[a], Zhongfang Zhao[e], Daniel B. Campbell[f], Leslie P. Weiner[f], and Wange Lu[a,2]

[a]The Eli and Edythe Broad Center for Regenerative Medicine and Stem Cell Research, University of Southern California, Los Angeles, CA 90033; [b]The Mork Family Department of Chemical Engineering and Materials Science, University of Southern California, Los Angeles, CA 90089; [c]Research Center, Dongnam Institute of Radiological and Medical Sciences, Busan 46033, South Korea; [d]Myung-Gok Eye Research Institute, Department of Medical Science, Konyang University, Daejeon 320-832, South Korea; [e]College of Life Sciences, Nankai University, Tianjin 300071, China; and [f]Zilkha Neurogenetic Institute, University of Southern California, Los Angeles, CA 90033

Edited by Andre M. Goffinet, University of Louvain, Brussels, Belgium, and accepted by Editorial Board Member Jeremy Nathans October 25, 2017 (received for review September 16, 2017)

**The receptor-like tyrosine kinase (Ryk), a Wnt receptor, is important for cell fate determination during corticogenesis. During neuronal differentiation, the Ryk intracellular domain (ICD) is cleaved. Cleavage of Ryk and nuclear translocation of Ryk-ICD are required for neuronal differentiation. However, the mechanism of translocation and how it regulates neuronal differentiation remain unclear. Here, we identified Smek1 and Smek2 as Ryk-ICD partners that regulate its nuclear localization and function together with Ryk-ICD in the nucleus through chromatin recruitment and gene transcription regulation. Smek1/2 double knockout mice displayed pronounced defects in the production of cortical neurons, especially interneurons, while the neural stem cell population increased. In addition, both Smek and Ryk-ICD bound to the Dlx1/2 intergenic regulator element and were involved in its transcriptional regulation. These findings demonstrate a mechanism of the Ryk signaling pathway in which Smek1/2 and Ryk-ICD work together to mediate neural cell fate during corticogenesis.**

neural stem cell | neurogenesis | Ryk signaling | noncanonical Wnt signaling

Wnt signaling pathways function in diverse biological processes during development (1, 2). Wnt signaling is essential in neurogenesis, but its downstream molecular mechanisms are still unclear (3). Although Wnt ligands and receptors are expressed in different patterns across the telencephalon during forebrain development (3, 4), canonical Wnt activity is first detected only in the dorsal telencephalon at embryonic day (E)8.5, and this activity gradually moves posteriorly to the cortical hem region (5, 6). This suggests that noncanonical Wnt signaling may play a major role in corticogenesis. Unlike canonical β-catenin–mediated Wnt signaling, little is known about how noncanonical Wnt signaling mediates its effects and how it interacts with other key signaling pathways during cortical development.

The related to receptor tyrosine kinase (Ryk) regulates many biological activities, including cell polarity (7), cell migration, axon guidance (8), skeletal development (9), cell fate determination (10), neurite outgrowth (11), and cortical neurogenesis (12). The extracellular part of Ryk comprises a Wnt inhibitory factor 1-like domain that enables its interaction with Wnt proteins. However, it is unclear how Ryk functions in response to Wnt signals. Ryk is an atypical member of the tyrosine kinase family, which has substitutions in its intracellular kinase subdomain. This substitution is predicted to affect its kinase activity. Studies have shown that Ryk does not have kinase activity both in vivo (13) and in vitro (14). Therefore, Ryk utilizes a unique mechanism to transduce extrinsic Wnt signaling to the nucleus.

We previously reported that, upon Wnt signaling stimulation, Ryk protein is cleaved by γ-secretase. The Ryk intracellular domain (Ryk-ICD) is released to the cytosol and then translocates to the nucleus upon Wnt signaling stimulation (7, 9, 12). When fused to a nuclear localization signal (NLS), Ryk-ICD is sufficient to rescue neuronal differentiation defects seen in *Ryk*$^{-/-}$ cells (12), suggesting that its nuclear localization is required for this function.

Ryk-ICD does not exhibit an apparent NLS, and therefore it is unclear how Ryk-ICD enters the nucleus to exert its effects on neuronal differentiation. In addition, it is unknown whether Ryk-ICD requires additional cofactors in the nucleus or in the chromatin to regulate neuronal differentiation.

Here, we identified that Smek1 and Smek2 (Smek1/2) are key factors in the Ryk signaling pathway. Smek1 is shown to promote neuronal differentiation in mouse neural stem cells with PP4C (15). Its *Drosophila* homolog, *flfl*, regulates the distribution of cell fate determination proteins during neuroblast asymmetric cell division (16). In this study, we discovered that Smek deficiency prevented neural stem cells from differentiating, thus leading to severe neurogenesis defects, including reduced interneuron formation. Most importantly, Ryk-ICD nuclear transport relied on Smek proteins. In the nucleus, Ryk-ICD and Smek cooccupied regulatory regions of neuronal genes and regulated their expression. Thus, we provide a molecular mechanism for mammalian

## Significance

**Receptor-like tyrosine kinase (Ryk) is a Wnt receptor and is important for many developmental processes, including cranial facial development, neurogenesis, and axon guidance. However, little is known about the role of the intracellular domain, Ryk-ICD, in signal transduction. Its downstream targets are also unknown. We have previously shown that Ryk-ICD is located in the cytoplasm of neural stem cells whereas it moves into the nucleus upon neuronal differentiation. In this study, we discovered that Smek1/2 function as a chaperone for Ryk-ICD during its nuclear localization and that both Smek and Ryk-ICD associate with chromatin to regulate the transcription of downstream target genes and neural differentiation.**

Author contributions: W.-H.C., S.H.C., and W.L. designed research; W.-H.C., S.H.C., B.-S.M., J.L., J.B., and I.H. performed research; W.-H.C., S.H.C., B.-S.M., M.C., J.L., F.G., Z.Z., D.B.C., and L.P.W. analyzed data; and W.-H.C. wrote the paper.

The authors declare no conflict of interest.

This article is a PNAS Direct Submission. A.M.G. is a guest editor invited by the Editorial Board.

Published under the PNAS license.

[1]W.-H.C. and S.H.C. contributed equally to this work.

[2]To whom correspondence may be addressed. Email: sihochoi@dirams.re.kr or wangelu@usc.edu.

This article contains supporting information online at www.pnas.org/lookup/suppl/doi:10.1073/pnas.1715772114/-/DCSupplemental.

neurogenesis, as well as further understanding of the noncanonical Wnt signaling pathway.

## Results

**Smek1 and Smek2 Are Ryk-Interacting Partners.** In our previous study, we reported that the Ryk receptor is cleaved at the transmembrane domain and that Ryk-ICD is translocated to the nucleus where it promotes neuronal differentiation (12). Since cleaved ICD does not exhibit an apparent NLS, we hypothesized that an NLS-containing protein may be required for the entry of Ryk-ICD into the nucleus. To identify potential coregulators, we performed a yeast two-hybrid screen using Ryk-ICD as the bait (Dataset S1). Among the 98 protein candidates identified in the assay, in addition to the known Ryk-interacting partner Cdc37 (17), Smek2 was one of the Ryk-interacting proteins.

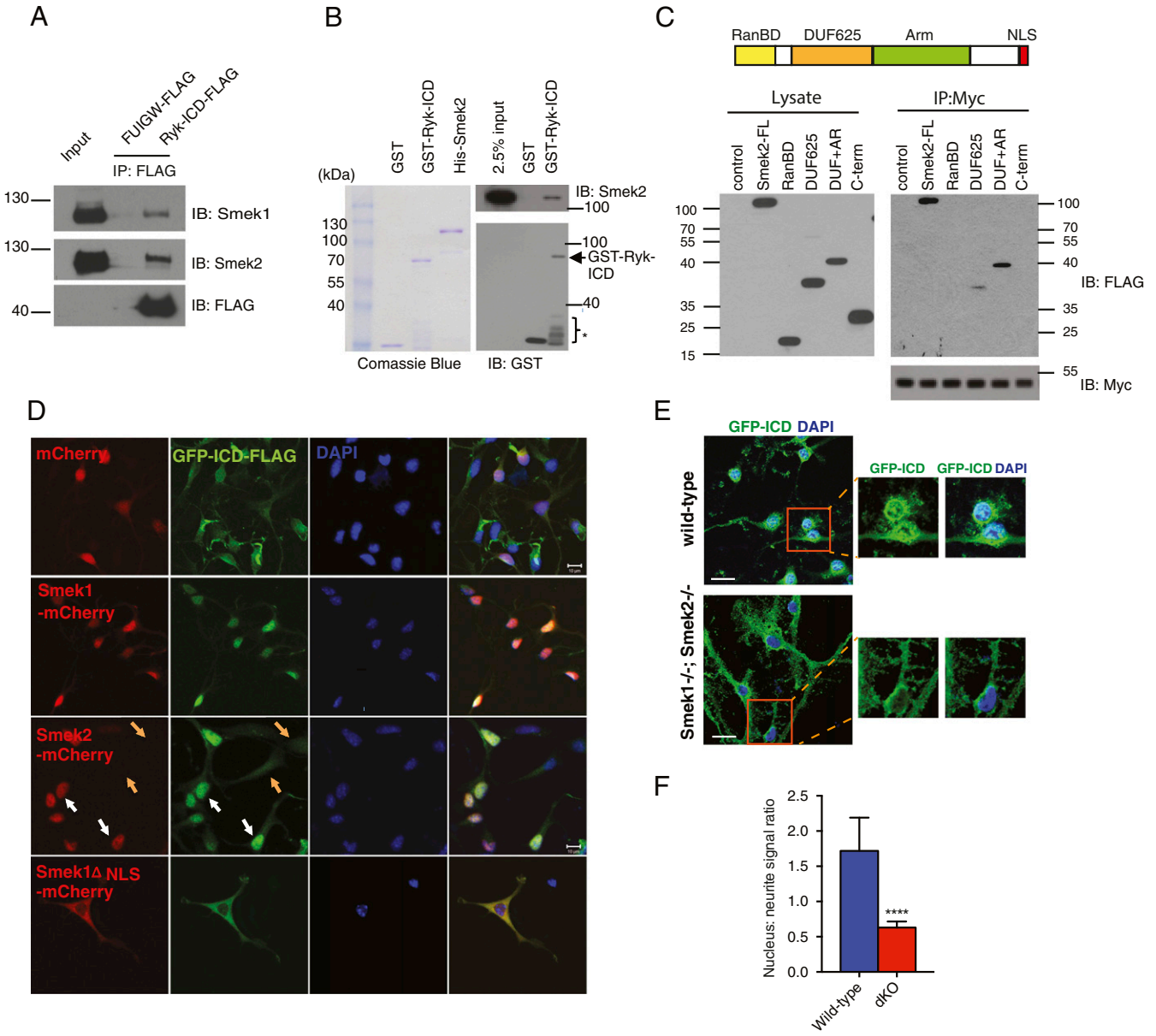


**Fig. 1.** Smek1 and Smek2 are identified as Ryk-interacting proteins, and Smek regulates Ryk nuclear translocation. (*A*) Ryk-ICD interacts with Smek1 and Smek2. Coimmunoprecipitation of overexpressed Ryk-ICD with Smek1 and Smek2 in HEK 293T cells. FUIGW-Flag serves as a negative control. IB, immunoblot. (*B*) Ryk-ICD binds Smek2 directly. (*Left*) Coomassie blue staining of purified GST, GST-tagged Ryk-ICD, and His-tagged Smek2. (*Right*) Immunoblot (IB) of the His-Smek2 and GST-tagged Ryk-ICD GST pull-down assay. The arrow indicates GST-tagged Ryk-ICD, and the asterisk indicates degraded GST-tagged Ryk-ICD. (*C*) Illustration of conserved domains of Smek protein. The Smek DUF domain mediates Ryk interaction. Immunoblot of the Myc-tagged Ryk and Flag-tagged Smek2 subdomains expressing HEK 293T cell lysate (*Left*), and immunoprecipitation assay with the FLAG antibody (*Right*). Arm, armadillo repeat region; DUF625, domain of unknown function 625; NLS, nuclear localization signal; RanBD, Ran-binding domain. (*D*) Mouse primary NSCs were infected with lentiviruses harboring mCherry only, Smek1-mCherry, Smek2-mCherry, Smek1ΔNLS-mCherry, or Ryk-ICD-GFP. White arrows indicate Smek1-mCherry–infected cells. Orange arrows indicate GFP-ICD–positive, Smek2-mCherry–negative cells. (Scale bars: 10 μm.) (*E*) Ryk-ICD nuclear localization is correlated with Smek1 expression. Doxycycline-inducible GFP-ICD-Flag lentiviruses were used to infect primary WT neural stem cells. Cells were stained against Smek1 antibody 2 d after doxycycline treatment under differentiation condition. Orange box *Inset* shows the location of the enlarged images on the right. (Scale bars: 20 μm.) (*F*) The average intensity of the cell nucleus and neurite was measured by ImageJ. The ratio of the nucleus area and neurite is shown here. [WT (n = 13), dKO ($n = 9$) ****$P < 0.0001$.]

The similarity score between Smek1 and Smek2 based on the T-Coffee alignment program (18) was 96, suggesting that these proteins might be functionally similar. Coimmunoprecipitation using extracts from stably expressing Ryk-ICD-FLAG HEK293T cells confirmed the interaction between Ryk-ICD and both Smek1 and Smek2 proteins (Fig. 1*A*). We also generated and purified GST-tagged Ryk-ICD and His-tagged Smek2 from bacteria and performed in vitro GST pull-down assays. Purified Ryk-ICD and Smek coimmunoprecipitated when incubated in vitro (Fig. 1*B*), suggesting that these two proteins directly interacted with each other.

Smek proteins contain four conserved domains: EVH-1 (RanBD), domain of unknown function (DUF625), armadillo repeat (Arm), and nuclear localization signal (NLS) (Fig. 1*C*). EVH-1 domains can localize proteins to F-actin–rich regions through interactions with polyproline substrates (19). The Smek EVH-1 domain is necessary for cytoplasmic/cortical localization whereas the NLS is responsible for its nuclear localization (20). To map the domains required for Ryk interaction, we generated constructs expressing FLAG-tagged Smek2 subdomains. Most subdomains were expressed in HEK293T cells, except for the armadillo-repeat only subdomain, which is likely unstable when expressed alone (Fig. 1 *C*, *Left*). FLAG-tagged Smek2 subdomains and Myc-tagged Ryk were cotransfected into HEK293 cells and immunoprecipitated with an anti-myc antibody. The EVH-1 domain and C terminus of Smek did not bind to Ryk (Fig. 1 *C*, *Right*). However, the Smek2 DUF domain alone bound to Ryk, indicating that the DUF domain is sufficient for Ryk binding. The interaction was enhanced by including the Smek2 armadillo repeat construct, indicating that either the armadillo repeat increased Ryk binding affinity or that the armadillo repeat alone could also bind to Ryk.

We then tested whether Ryk and Smek were expressed in the same sets of cells in vivo. We examined coronal sections of the cortex from $Ryk^{+/-}$ mice in which the *β-galactosidase* gene was used to replace the Ryk gene and *β-galactosidase* expression reflects endogenous *Ryk* gene expression (9). This is an alternative strategy for detecting the endogenous Ryk protein when lacking an available Ryk antibody. *β-galactosidase* was highly expressed in both the cortical plate (CP) and the ventricular zone (VZ), where neurons and cortical neural progenitor cells are located in vivo, respectively (Fig. S1*A*). Immunostaining with either Smek1 or Smek2 antibodies together with the *β-galactosidase* antibody confirmed that *Smek* expression overlapped with *Ryk* (*β-galactosidase*)-active populations in both the CP and VZ.

**Smek Proteins Facilitate Ryk-ICD Nuclear Localization.** To determine whether Smek proteins regulate Ryk-ICD nuclear localization, we generated mouse primary cortical neural stem cell (NSC) constitutively expressing GFP-Ryk-ICD and either the red fluorescent protein mCherry alone, or mCherry fused with Smek1 (mCherry-Smek1) or Smek2 (mCherry-Smek2). Each mCherry lentiviral construct was controlled by a doxycycline (dox)-inducible promoter. After dox treatment and induction of the mCherry control construct, we observed that Ryk-ICD protein distributed across the entire cell (Fig. 1*D*, first row). However, upon induction of mCherry-Smek1 or mCherry-Smek2, the GFP-Ryk-ICD signal

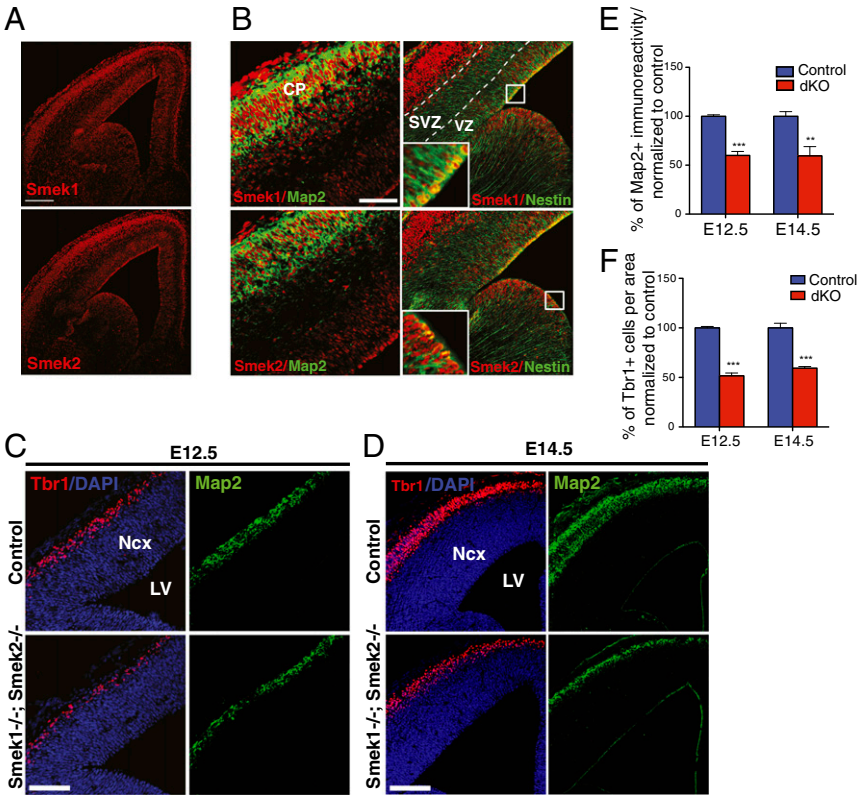


**Fig. 2.** *Smek1/2* play important roles in neurogenesis during cortical development. (*A*) Smek1 and Smek2 expression in E14.5 WT mouse brains. (Scale bar: 200 μm.) (*B*) Smek1 and Smek2 are expressed in both differentiated neurons and neural stem cells. Map2 marked neurons at the cortical plate (CP). Nestin marked neural stem cells at the ventricular zone (VZ) and subventricular zone (SVZ) of the dorsal and ventral telencephalon. White boxes indicate location of *Insets*. (Scale bar: 200 μm.) WT and $Smek1^{-/-}$; $Smek2^{-/-}$ mutant mouse E12.5 (*C*) and E14.5 (*D*) brain tissue was collected and stained for Tbr1 and Map2 expression. DAPI served as a nuclear stain. Quantification of *C* and *D* is shown in *E* and *F*, respectively. (*E*) The Map2 immunoreactivity in the whole-imaged area (0.36 $mm^2$) was measured and normalized to the value obtained from the control group. (*F*) $Tbr1^+$ cells in the whole-imaged area (0.36 $mm^2$) were counted and normalized to the value obtained from the control group. LV, left ventricle; Ncx, neocortex. (Scale bars: 100 μm.) Values represent the mean ± SEM (n = 3, $^{**}P < 0.01$, $^{***}P < 0.001$).

was detected in the nucleus in 2 to 3 h (Fig. 1*D*, second row, and third row, white arrows). In cells not transduced by mCherry-Smek1/2 constructs, the GFP-Ryk-ICD was detected throughout the cells (Fig. 1*D*, orange arrows). In addition, when an NLS deletion mutant mCherry-Smek1 construct was expressed, the GFP-Ryk-ICD signal was detected only in the cytoplasm (Fig. 1*D*, fourth row). These results indicate that expression of Smek led to nuclear localization of Ryk-ICD and that this effect required the Smek NLS.

To understand the dynamics of Ryk-ICD/Smek interaction and Ryk-ICD nuclear translocation, we performed live cell imaging using doxycycline-inducible Smek2 expression in NSCs. Following induction of mCherry-Smek2, we observed an mCherry signal within 2 h. Once mCherry-Smek2 became visible, GFP-Ryk-ICD was translocated into the nucleus (Fig. S1 *B* and *C* and Movie S1). In addition, we observed more nuclear Ryk-ICD expression in WT NSCs than *Smek1*$^{-/-}$; *Smek2*$^{-/-}$ [double knockout (dKO)] NSCs (Fig. 1 *E* and *F*). Doxycycline-inducible GFP-ICD-FLAG lentiviruses were transduced to NSCs for monitoring the ICD distribution. Cells were fixed and stained 2 d after doxycycline treatment under the differentiation condition. Moreover, subcellular fractionation of the cell extract followed by Western blotting indicated less nuclear entrance of Ryk-ICD in lysates from *Smek1*$^{-/-}$; *Smek2*$^{-/-}$ NSCs (Fig. S2) relative to control cells.

**Smek1 and Smek2 Knockout Mice Exhibited Defects in Neurogenesis.** To better understand the function of Smek1/2 in neurogenesis in vivo, we analyzed Smek1 and Smek2 double knockout mice. Smek1 and Smek2 knockout mice were generated (Fig. S3*A*) using *Smek1*$^{-/-}$ and *Smek2*$^{-/-}$ mutant ES cells in the C57BL/6 background. *Smek2* mRNA and protein expression were undetectable in *Smek2*$^{-/-}$ brain tissue by real-time quantitative PCR (RT-qPCR) (Fig. S3*B*) and Western blot analysis (Fig. S3 *C* and *D*); however, leaky expression of *Smek1* was detected in *Smek1*$^{-/-}$ tissue. *Smek1* expression was reduced to 45% and 20% of WT at the mRNA and protein level, respectively, an outcome potentially attributable to imperfect gene trapping. *Smek1*$^{-/-}$ mice (which we considered hypomorphic) or *Smek2*$^{-/-}$ mice were born at normal Mendelian ratios, were viable and fertile, and did not differ in gross morphology from WT littermates. However, the viability of *Smek1/2* double knockout mice was dramatically compromised. A $\chi^2$ test was performed on the numbers of embryos obtained at different stages (Fig. S3 *E*–*G*). Although we obtained Smek double mutant embryos at E12.5 at a normal Mendelian ratio ($P$ = 0.3, insignificant compared with the expected ratio), by E14.5, the

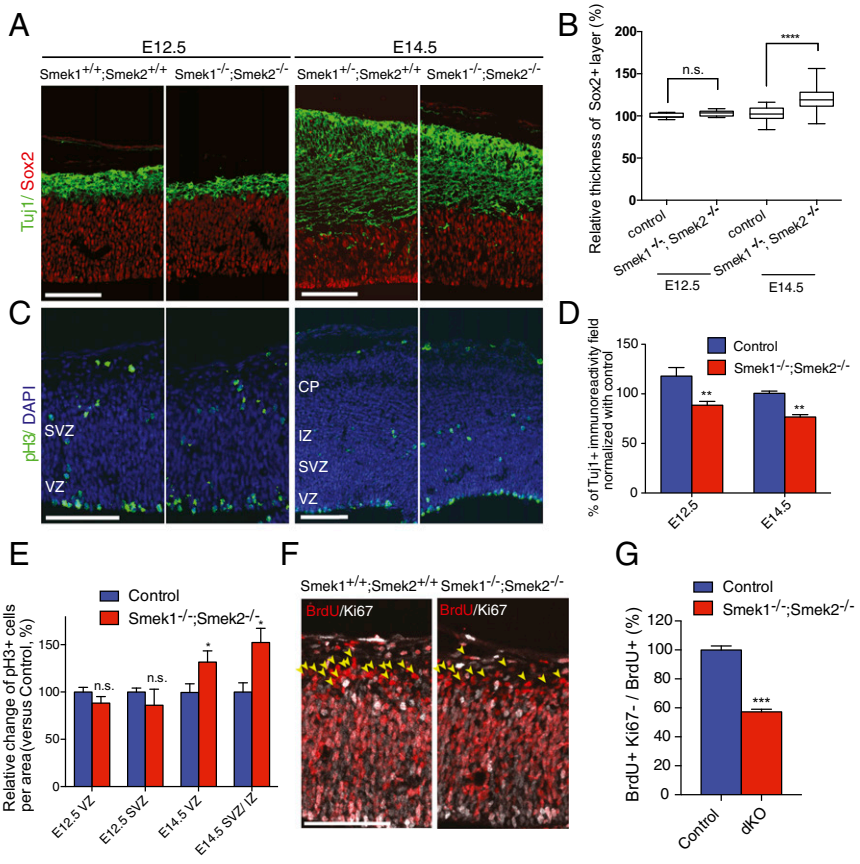


**Fig. 3.** Smek deficiency restricts NSC differentiation and causes neurogenesis defect. E12.5 and E14.5 mouse brain coronal sections from control and *Smek1*$^{-/-}$; *Smek2*$^{-/-}$ mice stained with Sox2 and Tuj1 (*A*), Phospho-Histone H3 (pH3) (*C*), BrdU (*F*), Ki67 (*F*) antibody, respectively. *Smek1*$^{+/+}$; *Smek2*$^{+/+}$, *Smek1*$^{+/-}$; *Smek2*$^{+/+}$, and *Smek1*$^{+/+}$; *Smek2*$^{+/-}$ mice all served as control mice. Cell nuclei were stained with DAPI. (*B*) Quantification of Sox2$^{+}$ cells by measuring the thickness of the Sox2$^{+}$ layer relative to the whole cortex. Four measurements were taken on each image. Values represent mean ± SEM ($n$ = 3; ****$P$ < 0.0001; n.s., not statistically significant). (*D*) Quantification of Tuj1$^{+}$ immunoreactivity area normalized to control ($n$ = 3, **$P$ < 0.01, Student's $t$ test). (*E*) Quantification of pH3$^{+}$ cells per area (0.36 mm$^2$) relative to control. VZ and SVZ/IZ were analyzed separately ($n$ = 3; n.s., not statistically significant; *$P$ < 0.1). (*F*) Cell cycle exit assay showed that Smek deficiency keeps NSCs from exiting the cell cycle. A BrdU pulse was administered 24 h before embryo collection at E12.5. BrdU$^{+}$Ki67$^{-}$ cells (yellow arrowhead) marked that the cell population left the cell cycle in 24 h. (Scale bar: 100 μm.) (*G*) Quantification of (*F*) BrdU$^{+}$Ki67$^{-}$ cells in each image field (0.72 mm$^2$) were counted and normalized to BrdU$^{+}$ cells ($n$ = 3, ***$P$ < 0.001). CP, cortical plate; IZ, intermediate zone; SVZ, subventricular zone; VZ, ventricular zone.

double mutant embryo number significantly decreased, and no Smek double mutant embryos were viable at the later stages. Thus, we only analyzed the *Smek1*$^{-/-}$*; Smek2*$^{-/-}$ embryos at the early-mid neurogenesis stage (E12.5 and E14.5).

To investigate the role of Smek in the developing mouse cortex, we first performed immunostaining on cryostat sections of brains collected from WT E14.5 mouse embryos. Smek1- and Smek2-positive–stained cells were labeled by neuronal marker Map2 in the CP and by neural stem cell marker Nestin in the VZ and subventricular zone (SVZ) (Fig. 2 *A* and *B*), suggesting that Smek1/2 were expressed in neural stem cells and neurons.

*Ryk*$^{-/-}$ mice exhibit defects in forebrain cortical neuronal differentiation (12) and GABAergic neuron formation (10). To determine whether *Smek1/2* deletion exhibits similar neurogenesis defects, the sections of control and *Smek1*$^{-/-}$*; Smek2*$^{-/-}$ brains collected at E12.5 and E14.5 were stained with a series of markers. The significant decreases in the numbers of Map2$^{+}$, Tbr1$^{+}$, and Tuj1$^{+}$ cells indicated the loss of neurons in the Smek-deficient embryos (Figs. 2 *C–F* and 3 *A* and *D*). Undetectable differences in the TUNEL analysis (Fig. S4 *A* and *B*) suggested that cell apoptosis did not contribute to the neuron loss.

**Smek1/2 Double Knockout Mice Had More Neural Stem Cells than Control Mice.** We then checked whether the progenitor cell population was affected by Smek1/2 deficiency. The Sox2 antibody was used to label the neural stem cells (Fig. 3 *A* and *B*). Interestingly, the Sox2$^{+}$ cell layer in the Neocortex (NCx) was thicker in the *Smek1*$^{-/-}$*; Smek2*$^{-/-}$ E14.5 embryo than in the WT control. Such a difference was not observed at the earlier stage (E12.5). To monitor actively proliferating cells, phospho-Histone H3 (pH3) staining (Fig. 3 *C* and *E*) and short-pulse BrdU labeling (Fig. S4 *C* and *D*) was performed at both stages. The proliferating cell population at the E14.5 stage was greater in the Smek-deficient mice than in the control mice.

Although there were not more proliferating cells in Smek-deficient mice at E12.5, lineage-tracing experiments showed that fewer cells exited the cell cycle. Injection of BrdU 24 h before embryo collection enabled us to trace the progenitor cell fate (Fig. 3 *F* and *G*). When the brain sections were stained with Tbr2 antibody, an intermediate progenitor marker, fewer Tbr2$^{+}$ cells were detected at the earlier stage of the Smek1/2-deficient embryos (Fig. S4 *E* and *F*). Together, these observations suggest that, without the Smek proteins, neural progenitor cell differentiation is delayed. Smek influenced the transition of radial glial cells to intermediate progenitor cells at the earlier stage and then eventually affected neurogenesis.

**Smek1/2 Regulate GABAergic Cortical Interneuron Neurogenesis.** Ryk knockout mice also exhibited defects in GABAergic neuron formation (10). Therefore, we next examined the distribution of GABAergic interneurons in vivo. At E14.5, GABAergic neurons are generated from the medial ganglionic eminence (MGE) and migrate either radially to the neocortex or hippocampus, or tangentially to the piriform cortex and deeper striatum (21). All Dlx2$^{+}$ GABAergic cells are Smek1$^{+}$ and Smek2$^{+}$ cells on the tangential migration path to the neocortex and hippocampus in the WT mice (Fig. 4*A*). In the Smek double mutant mice, Dlx2$^{+}$ cell populations in both neocortex and piriform cortex were significantly reduced (Fig. 4 *B* and *D*). Using another GABAergic marker, calbindin, we found that the number of calbindin$^{+}$ cells at E12.5 and E14.5 were reduced in Smek double mutant mice compared to the control mice (Fig. 4 *C* and *E*). These data indicate that loss of Smek proteins led to severely impaired GABAergic neurogenesis in vivo, a phenotype similar to Ryk knockout mice.

**Genome-Wide Identification of Genes Influenced by *Smek1/2* Deficiency.** To obtain a global view of the genes regulated by Smek1/2, we

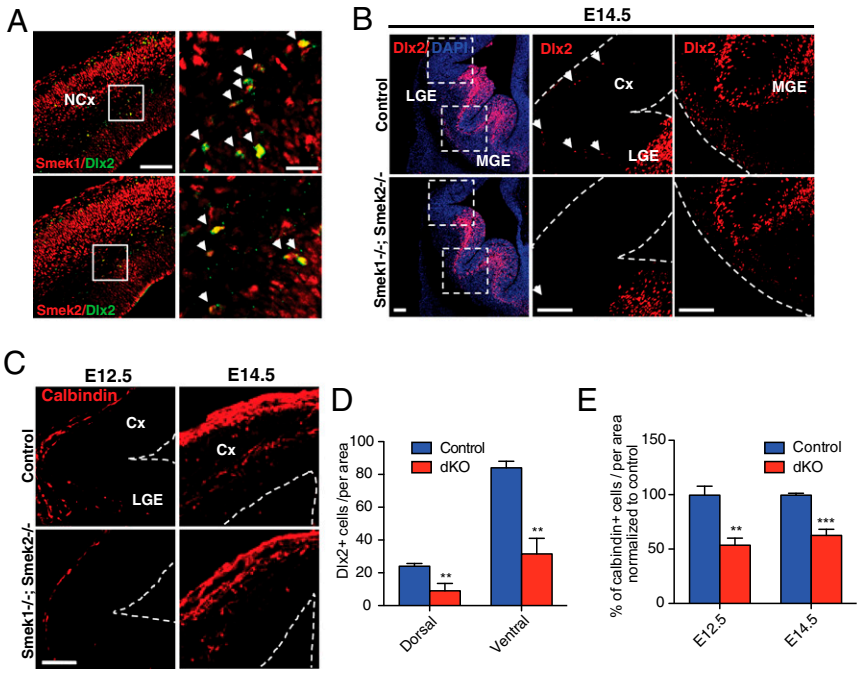


**Fig. 4.** Smek1/2 controls GABAergic neurogenesis by direct regulation of Dlx gene expression. (*A*) Coronal sections of E14.5 WT cortex stained with Smek1, Smek2, or Dlx2 antibody. Dlx2 marks migrating GABAergic neurons in the neocortex. The close-up *Inset* shows that all of the Dlx2 staining overlaps with Smek staining. White arrow indicates cells that show both Smek and Dlx2 positive staining. NCx, neocortex. (*B*) Dlx2 staining showed a decrease of GABAergic neurons in Smek-deficient mice. White arrowheads indicate tangentially migrating Dlx2$^{+}$ interneurons. Quantification is shown in *D*. Cx, cortex; LGE, lateral ganglionic eminence; MGE, medial ganglionic eminence. (*C*) Smek-deficient mice showed less calbindin$^{+}$ cells at both E12.5 and E14.5 stage. Quantification is shown in *E*. (Scale bars: A, 100 μm, 50 μm; *B*, 50 μm, 100 μm, 100 μm; *C*, 100 μm.) Values represent mean ± SEM ($n = 3$, $^{**}P < 0.01$, $^{***}P < 0.001$).

performed RNA-seq on WT and *Smek1*$^{-/-}$; *Smek2*$^{-/-}$ NSCs that underwent differentiation for 2 d. A hierarchical clustering heat map was generated with a list of differentially expressed genes (575 in total) in mutant versus control samples using Cuffdiff with a false discovery rate (FDR) ≤ 0.05 (Fig. S5*A*). Control and mutant samples were clustered, respectively, and had distinct expression patterns. As expected, the important neurogenesis regulators, such as *Eomes*, *Myt1l*, *Gsx1*, *Bcl11b (Ctip2)*, and *Neurod2*, were significantly down-regulated (Fig. 5*A*). Neural progenitor markers *Otx2*, *Six3*, *En2*, and *Lmx1a* were up-regulated, being consistently the phenotype of NSC accumulation in vivo. In addition, GABAergic neuron specification genes, including *Dlx1*, *Dlx1as*, *Dlx2*, and *Calb2*, were also all robustly down-regulated.

The genes down-regulated by fold change value of ≥1.5 in double mutant cells were further analyzed with ingenuity pathway analysis (IPA) (Fig. 5*B*). In the disease and biofunction annotations, development of the head, formation of the brain, development of neurons, and proliferation of cells annotation terms were on the top-10-gene list, highlighting the important roles of Smek proteins during nervous system development.

**Genome-Wide Identification of Smek Binding Sites.** In mouse embryonic stem cells (mESCs), Smek forms a transcription regulatory complex with HDAC1 and PP4C to the *brachyury* promoter and inhibits *brachyury* expression (22). This suggests the possibility of Smek being directly involved in transcriptional regulation even though Smek protein does not carry any conserved DNA binding domains. To identify downstream targets of Smek1 in NSCs, we performed chromatin immunoprecipitation, followed by high-throughput sequencing (ChIP-seq) with a Smek1 antibody in primary mouse NSCs. (ChIP-seq was not performed for Smek2 due to the lack of a ChIP-grade Smek2 antibody.) Smek1 bound to the regulatory regions of transcription factors known to drive neural cell fate, such as *Dlx1*, *Dlx1as*, *En1*, *Irx3*, *Otx1*, and *Sp9* (Fig. 5*C*). The gene ontology (GO) analysis result of the list of Smek1 binding genes highly correlated with central nervous system development and neurogenesis (Fig. 5*D*), in agreement with Smek1/2 double knockout phenotypes.

Interestingly, when Smek1 binding sites were annotated to the genome, the binding sites were distributed largely in the promoters (37.8%) and 5′ UTR (12.2%). It showed a distinct binding profile, compared with the genome annotation profile (>90% intron and distal intergenic region), suggesting a possible role of Smek1 in transcriptional regulation (Fig. S5*B*). Among 23,420 genes included in this analysis, 1,259 were bound by Smek1. Among them, 30 had a significantly different expression in control and Smek1/2 double knockout (dKO) cells. A hierarchical clustering heat map was generated (Fig. S5*C*) using these genes. Among these genes, the neuronal genes showed lower expression levels, and the neural progenitor genes showed higher expression levels in the Smek1/2 double knockout cells. This expression profile matched the in vivo phenotypes in the Smek double knockout embryos.

**Ryk and Smek Work Together to Regulate Neurogenesis.** To determine whether Ryk-ICD and Smek1 work together after translocation into the nucleus for transcriptional regulation, we

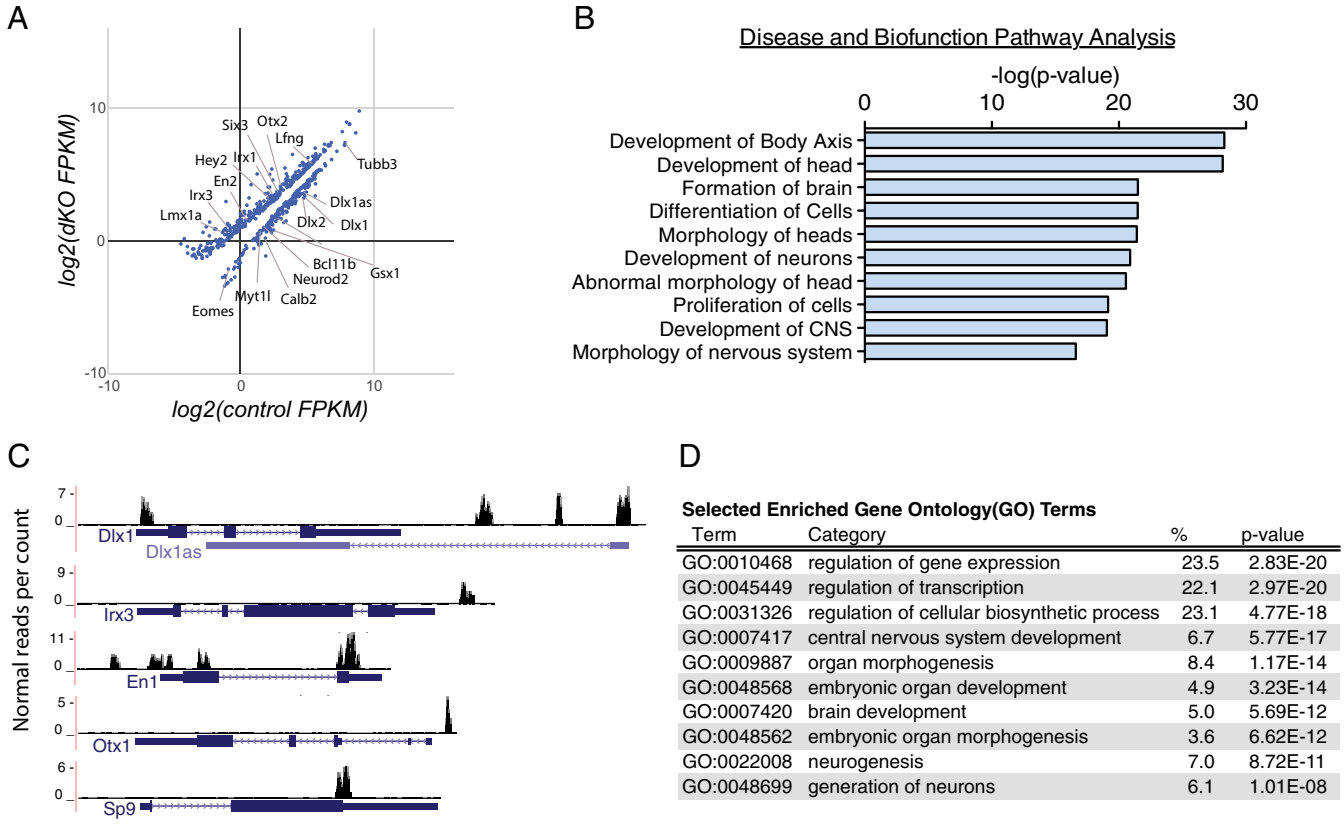


**Selected Enriched Gene Ontology(GO) Terms**

| Term | Category | % | p-value |
|---|---|---|---|
| GO:0010468 | regulation of gene expression | 23.5 | 2.83E-20 |
| GO:0045449 | regulation of transcription | 22.1 | 2.97E-20 |
| GO:0031326 | regulation of cellular biosynthetic process | 23.1 | 4.77E-18 |
| GO:0007417 | central nervous system development | 6.7 | 5.77E-17 |
| GO:0009887 | organ morphogenesis | 8.4 | 1.17E-14 |
| GO:0048568 | embryonic organ development | 4.9 | 3.23E-14 |
| GO:0007420 | brain development | 5.0 | 5.69E-12 |
| GO:0048562 | embryonic organ morphogenesis | 3.6 | 6.62E-12 |
| GO:0022008 | neurogenesis | 7.0 | 8.72E-11 |
| GO:0048699 | generation of neurons | 6.1 | 1.01E-08 |

**Fig. 5.** Genome-wide Smek binding sites and expression profiling of Smek-deficient NSCs. (*A*) Scatter plot of significantly changed genes from RNA sequencing results. Several important neuronal genes were handpicked and labeled. Three pairs of control and *Smek1*$^{-/-}$; *Smek2*$^{-/-}$ NSCs were differentiated for 2 d before RNA extraction, followed by sequencing library preparation. (*B*) Top 10 IPA annotations of the disease and biofunction of the genes decreased more than twofold in *Smek1*$^{-/-}$; *Smek2*$^{-/-}$ cells relative to controls (q ≤ 0.5). (*C*) Selected Smek1 binding tracks (ChIP-seq) on the University of California, Santa Cruz (UCSC) Genome Browser. (*D*) Selected enriched GO terms were generated from the list of Smek1 binding genes using the Database for Annotation, Visualization and Integrated Discovery (DAVID) Bioinformatics online tool. FPKM, fragments per kilobase of transcript per million mapped reads.

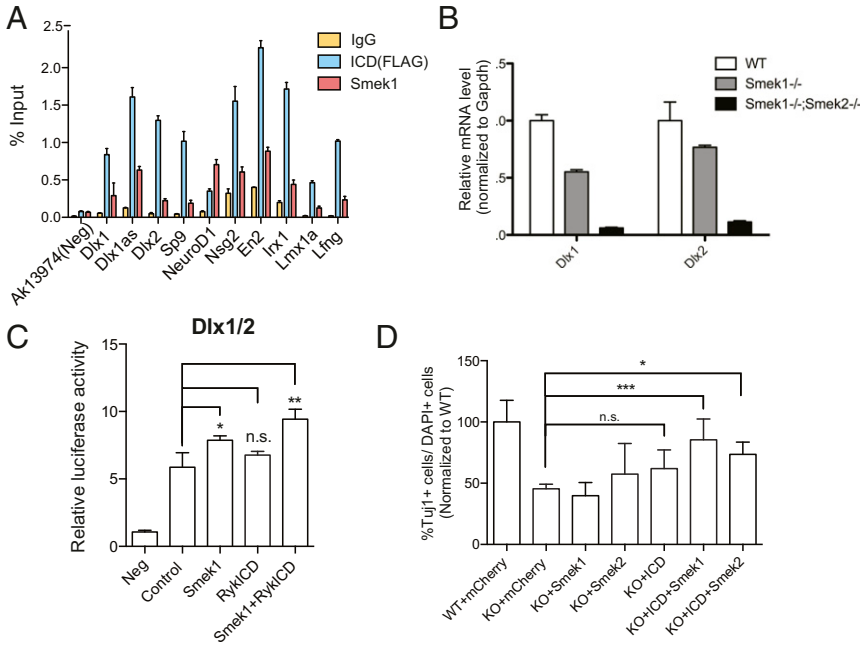


**Fig. 6.** Ryk-ICD is recruited to the downstream target genes and Ryk functions with Smek to regulate neurogenesis. (*A*) Ryk-ICD and Smek1 bind to some similar genomic loci. ChIP-qPCR was performed with FLAG and Smek1 antibody using the FLAG knockin cell line. Primer sets were designed based on the Smek1 ChIP-seq result. (*B*) Real-time PCR of Dlx1 and Dlx2 transcripts in NSCs from WT, Smek1$^{-/-}$, and Smek1$^{-/-}$; Smek2$^{-/-}$ mice. Relative mRNA expression levels are normalized to Gapdh. (*C*) Smek1 and Ryk-ICD regulate Dlx1/2 transcription activity. The Dlx1/2 intergenic regulatory region was cloned into the pGL3.Basic luciferase reporter. Control vector (FUGW), Smek1, Ryk-ICD, β-galactosidase reporter, and the Dlx1/2 reporter were cotransfected into HEK293T cells. Luciferase activity was normalized to β-galactosidase activity in each condition and then normalized to the "Neg" condition. Neg, the experimental group, which was only transfected with β-galactosidase reporter and control vector. Values represent mean ± SEM ($n = 3$; $^*P < 0.1$; $^{**}P < 0.01$; n.s., not significant; unpaired *t* test). (*D*) Coexpression of ICD and Smek rescue neurogenesis defect in Ryk$^{-/-}$ NSCs. Ryk$^{+/+}$ (WT) and Ryk$^{-/-}$ (KO) NSCs were transduced with lentiviruses expressing GFP (FUGW), ICD-GFP, mCherry, Smek1-mCherry, and Smek2-mCherry. Cells were allowed to differentiate for 2 d and were stained with Tuj1. Quantification of neurons is presented by the percentage of Tuj$^+$ mCherry$^+$ GFP$^+$ cells among mCherry$^+$ GFP$^+$ cells. Values represent mean ± SEM in independent cell lines ($n = 3$, one-way ANOVA, $P < 0.0001$; post hoc *t* test results are labeled on the graph as $^*P < 0.05$, $^{***}P < 0.001$,; n.s., not significant).

performed ChIP-qPCR analysis to test Ryk-ICD binding at the chromatin. Due to the lack of a Ryk-ICD antibody, a peptide of three-FLAG tag was added to the endogenous Ryk protein using CRISPR technology (Fig. 6*A* and Fig. S6) in mESCs, which were then differentiated into NSCs. The binding loci of Ryk-ICD and Smek1 were identified by chromatin immunoprecipitation using the FLAG antibody and the Smek1 antibody, respectively. qPCR primers were designed based on the previous Smek1 ChIP-seq result. Interestingly, Ryk-ICD bound to most of the Smek1 binding regions, indicating the possibility of being in the same coregulator complex.

To determine whether Ryk-ICD and Smek directly affect gene transcription, we constructed a Dlx1/2 intergenic region luciferase reporter. This intergenic region has been reported as the key regulatory element for both *Dlx1* and *Dlx2* genes (23). ChIP-seq and ChIP-qPCR proved that Smek associated with this region. Smek1 and 2 were also found to be required for expression of *Dlx1* and *Dlx2*. RT-qPCR analysis using WT, *Smek1*$^{-/-}$, and *Smek1*$^{-/-}$; *Smek2*$^{-/-}$ NSCs demonstrated that *Dlx1* and *Dlx2* mRNA levels were lower in *Smek1* single knockout and even lower in *Smek1/2* double knockout NSCs (Fig. 6*B*).

A luciferase assay using the Dlx1/2 intergenic region demonstrated that Dlx1/2 reporter activity was slightly elevated with Smek1 overexpression and significantly increased when both Smek1 and Ryk-ICD were cooverexpressed (Fig. 6*C*). These results show that Ryk-ICD and Smek1 may play a positive role in regulating transcription.

To determine whether Smek and Ryk require each other to regulate neurogenesis, *Ryk*$^{+/+}$ (WT) and *Ryk*$^{-/-}$ (KO) NSCs were transduced with lentiviruses expressing GFP, Ryk-ICD-GFP, and dox-inducible mCherry, Smek1-mCherry, or Smek2-mCherry (Fig. 6*D*). We observed a very significant defect in neuronal differentiation in *Ryk*$^{-/-}$ NSCs, and overexpression of Smek1 or Smek2 could not rescue the neuronal differentiation phenotype of *Ryk*$^{-/-}$ NSCs. Putting back Ryk-ICD increased the Tuj1$^+$mCherry$^+$ numbers in a small degree. The reason that Ryk-ICD alone could not rescue the neural differentiation may be that not enough endogenous Smek protein was present to shuttle Ryk-ICD into the nucleus. The Smek1/2 expression level was indeed lower in the Ryk$^{-/-}$ NSCs (Fig. S7). Hence, only when Smek1 or Smek2 was cotransduced together with Ryk-ICD into *Ryk*$^{-/-}$ NSCs were Tuj1$^+$ mCherry$^+$ neuron numbers similar to the WT control. Thus, Ryk and Smek proteins were both required for neuronal differentiation and acted together to regulate transcription and neuronal differentiation.

## Discussion

We previously discovered that the noncanonical Wnt receptor Ryk plays an important role in determining neural cell fate (10, 12). While the canonical Wnt pathway is well understood, very little is known about the Wnt/Ryk signal transduction pathway. Upon Wnt binding, an increased amount of Ryk-ICD translocates into the nucleus whereas the total Ryk protein level is not affected (20). However, lacking a nuclear localization signal, it was unclear how Ryk-ICD enters the nucleus. Our results demonstrate that Smek interacts with Ryk-ICD and translocates Ryk-ICD into the nucleus. The live-cell imaging assay clearly showed that Ryk-ICD translocation was highly dependent on Smek proteins and that the translocation occurred rapidly after Smek expression. A significantly smaller amount of Ryk-ICD entered

the Smek-deficient cell nucleus. Thus, Smek proteins are critical for mediating Ryk-ICD nuclear translocation.

In addition to shuttling Ryk-ICD into the nucleus, Smek proteins interact with Ryk in the nucleus, and they are involved in transcriptional regulation. Our ChIP-seq and ChIP-qPCR results show that Smek1 bound to loci containing genes required for neural cell fate determination. Many of the gene loci were also bound by Ryk-ICD. The fact that the Smek1/Ryk-ICD binding profiles were strongly correlated with transcriptome analysis indicates that these binding events are involved in regulating transcription. In further support of this notion, *Smek1/2* double knockout led to reduced expression of some Smek1 target genes identified by ChIP-seq analysis. Gene expression of GABAergic neuron lineage factors, *Dlx1*, *Dlx1as*, *Dlx2*, and *Calb2*, was impaired and so was this neuron population. A luciferase reporter assay also showed the direct transcriptional activity changes of the Dlx1/2 intergenic region by Smek1 and Ryk-ICD proteins. Thus, Smek-dependent translocation of Ryk-ICD and the Smek/Ryk coregulation of transcription in the nucleus represent a noncanonical Wnt signaling pathway that regulates neuronal differentiation of stem cells.

Wnt signaling is dynamic throughout developmental processes. Wnt ligands and receptors are expressed in spatiotemporal patterns in different regions. During forebrain development, canonical Wnt activity is highly restricted. It is only detected first in the dorsal telencephalon at E8.5, and it gradually becomes restricted to the cortical hem (6). Thus, β-catenin–independent Wnt signaling must play a large part in cortical neurogenesis. Here, we identified the Ryk/Smek signal as a critical player in the intricate signaling network during corticogenesis.

Ryk like Notch is cleaved at the transmembrane region by the γ-secretase complex, and it releases the intracellular domain from the cell membrane. However, Notch-ICD and Ryk-ICD then use distinct protein partners to regulate downstream targets. Notch-ICD forms transcription complexes with DNA binding proteins and other coregulators (such as RBP-J, Maml-1) to regulate gene expression and stem cell renewal (24) while Ryk-ICD forms a complex with Smek to regulate gene expression and cell differentiation. Ryk-ICD and Notch-ICD not only use a discrete pathway to regulate different gene expression, but these two pathways may cross-talk to orchestrate gene expression to determine neural stem cell self-renewal and differentiation. Our previous study identified Par3 as a substrate of the Smek1/PP4c complex during neuronal differentiation (15). The Par3/aPKC complex is an upstream effector of Notch signaling. Dephosphorylation of Par3 would activate Numb activity, which inhibits the Notch signaling pathway, hence leading to neuron differentiation (25). It is possible that Smek may be a key player for cross-talk of the Wnt/Ryk and Notch pathways.

Our study has revealed a noncanonical Wnt signal transduction pathway mediated by the Ryk receptor. This study delineates how extrinsic signals are transduced from the membrane to the nucleus to regulate gene expression and neuronal cell fate.

## Materials and Methods

**Cell Culture, Cortical Neural Stem Cell Derivation, and Neuronal Differentiation.** HEK293T cells were maintained in DMEM (Cellgro) with 10% FBS (HyClone) and 1% Pen/Strep (Caisson). E14 mouse embryonic stem cells (mESCs) were cultured in mouse ES medium [GMEM, 15% FBS, nonessential amino acid, L-glutamine, β-mercaptoethanol, pen/strep, and leukemia inhibitory factor (LIF) generated from engineered Chinese hamster ovary(CHO) cells]. Primary cortical neural stem cells were derived from E11.5 mouse embryos and maintained in neural stem cell medium [DMEM/F-12 (Cellgro) with 1× B27 supplement (Gibco), 1% Pen/Strep, and 20 ng/mL basic fibroblast growth factor (bFGF) (Gibco)]. The method of derivation was similar to what has been previously described (10). Briefly, cortices were dissected from E11.5 mouse embryos and dissociated to single cells with 0.05% Trypsin (Caisson). Dissociated cells were then plated onto poly-L-ornithine (Sigma-Aldrich) and Fibronectin (Gibco)-coated plates in culture medium. Neuronal differentiation was initiated by withdrawal of bFGF from the medium. The NSCs were seeded on coverslips overnight and then switched to differentiation conditions with the addition of dox to induce mCherry or Smek-mCherry expression. In vitro differentiation of NSCs from mouse ES cells was performed as described previously (26).

**Generation of Ryk Knockin Cell Line with CRISPR Technology.** We designed a donor plasmid carrying homology arms of C terminus of Ryk protein and three FLAG, Biotin, GFP, and phosphoglycerate kinase (PGK) promoter-driven drug selection cassettes (neomycinR) flanked by loxP sites. When the homologous recombination happened via dCas9 and two guide RNAs (gRNAs) specifically targeting Ryk loci, the cells would have GFP and drug resistance. The CRISPR Genome Editing Resource online tool was used for designing gRNAs. Five gRNAs were picked and cloned into the pX335 plasmid. Only one pair of gRNAs generated knockin (KI) cells successfully. gRNA1-TTTCTTCTGAGTGGCGGAGCTGG, gRNA5-AAGAAAGTGCCTGTCTGTCACGG Amaxa Nucleofector, and the mouse ESC Nucleofector Kit (Lonza) were used for transfection. The transfected cells were selected with neomycin for 5 d before being sorted by using flow cytometry (Fig. S6*A*), and the cells with green fluorescence were kept (mESC 201G). Primers were designed for detecting WT and knockin (KI) mutant alleles (Fig. S6*B*), and then mutant cell lines generated from single clones were used for the following experiments (Fig. S6*C*).

**BrdU Labeling and Cell Cycle Exit Assay.** Labeling was performed using the method of Wojtowicz et al. (27). Briefly, actively proliferating cells were labeled with 100 mg·kg$^{-1}$ BrdU (Sigma-Aldrich) injected intraperitoneally 30 min before collecting mouse embryos.

For the cell cycle exit assay, a similar strategy was utilized, but BrdU was injected 24 h before mice were killed. Immunostaining was performed with anti-BrdU and anti-ki67 antibodies. We used the following formula to calculate the percentage of cells that had exited the cell cycle: [(total BrdU$^+$ cells) – (BrdU$^+$ki67$^+$ cells)]/total BrdU$^+$ cells.

**Statistical Analysis.** For all quantifications, at least three mice were collected for each genotype (plus control littermates), and more than three brain sections were collected from each mouse. Statistical analysis was done using Student's *t* tests or one-way ANOVA depending on experiment settings. A $\chi^2$ analysis was performed on the number of embryos we collected.

Additional methods are described in *SI Experimental Procedures*.

**ACKNOWLEDGMENTS.** This work was supported by US NIH Grant R01 NS067213-01A1 (to W.L.), Dongnam Institute of Radiological and Medical Sciences (DIRAMS) Grant 50590-2017 funded by the Korean government, Ministry of Science and ICT (MSIT) (to S.H.C.), and National Natural Science Foundation of China Grant 31530027 (to Z.Z.).

1. Moon RT, Kohn AD, De Ferrari GV, Kaykas A (2004) WNT and beta-catenin signalling: Diseases and therapies. *Nat Rev Genet* 5:691–701.
2. Klaus A, Birchmeier W (2008) Wnt signalling and its impact on development and cancer. *Nat Rev Cancer* 8:387–398.
3. Bielen H, Houart C (2014) The Wnt cries many: Wnt regulation of neurogenesis through tissue patterning, proliferation, and asymmetric cell division. *Dev Neurobiol* 74:772–780.
4. Shimogori T, Banuchi V, Ng HY, Strauss JB, Grove EA (2004) Embryonic signaling centers expressing BMP, WNT and FGF proteins interact to pattern the cerebral cortex. *Development* 131:5639–5647.
5. Harrison-Uy SJ, Pleasure SJ (2012) Wnt signaling and forebrain development. *Cold Spring Harb Perspect Biol* 4:a008094.
6. Machon O, et al. (2007) A dynamic gradient of Wnt signaling controls initiation of neurogenesis in the mammalian cortex and cellular specification in the hippocampus. *Dev Biol* 311:223–237.
7. Andre P, et al. (2012) The Wnt coreceptor Ryk regulates Wnt/planar cell polarity by modulating the degradation of the core planar cell polarity component Vangl2. *J Biol Chem* 287:44518–44525.
8. Keeble TR, Cooper HM (2006) Ryk: A novel Wnt receptor regulating axon pathfinding. *Int J Biochem Cell Biol* 38:2011–2017.
9. Halford MM, et al. (2000) Ryk-deficient mice exhibit craniofacial defects associated with perturbed Eph receptor crosstalk. *Nat Genet* 25:414–418.
10. Zhong J, et al. (2011) The Wnt receptor Ryk controls specification of GABAergic neurons versus oligodendrocytes during telencephalon development. *Development* 138:409–419.
11. Lu W, Yamamoto V, Ortega B, Baltimore D (2004) Mammalian Ryk is a Wnt coreceptor required for stimulation of neurite outgrowth. *Cell* 119:97–108.
12. Lyu J, Yamamoto V, Lu W (2008) Cleavage of the Wnt receptor Ryk regulates neuronal differentiation during cortical neurogenesis. *Dev Cell* 15:773–780.

13. Yoshikawa S, Bonkowsky JL, Kokel M, Shyn S, Thomas JB (2001) The derailed guidance receptor does not require kinase activity in vivo. *J Neurosci* 21:RC119.
14. Inoue T, et al. (2004) C. elegans LIN-18 is a Ryk ortholog and functions in parallel to LIN-17/Frizzled in Wnt signaling. *Cell* 118:795–806.
15. Lyu J, et al. (2013) Protein phosphatase 4 and Smek complex negatively regulate Par3 and promote neuronal differentiation of neural stem/progenitor cells. *Cell Rep* 5:593–600.
16. Sousa-Nunes R, Chia W, Somers WG (2009) Protein phosphatase 4 mediates localization of the Miranda complex during Drosophila neuroblast asymmetric divisions. *Genes Dev* 23:359–372.
17. Lyu J, Wesselschmidt RL, Lu W (2009) Cdc37 regulates Ryk signaling by stabilizing the cleaved Ryk intracellular domain. *J Biol Chem* 284:12940–12948.
18. Di Tommaso P, et al. (2011) T-Coffee: A web server for the multiple sequence alignment of protein and RNA sequences using structural information and homology extension. *Nucleic Acids Res* 39:W13–W17.
19. Renfranz PJ, Beckerle MC (2002) Doing (F/L)PPPPs: EVH1 domains and their proline-rich partners in cell polarity and migration. *Curr Opin Cell Biol* 14:88–103.
20. Mendoza MC, et al. (2005) Loss of SMEK, a novel, conserved protein, suppresses MEK1 null cell polarity, chemotaxis, and gene expression defects. *Mol Cell Biol* 25:7839–7853.
21. Marín O, Rubenstein JL (2001) A long, remarkable journey: Tangential migration in the telencephalon. *Nat Rev Neurosci* 2:780–790.
22. Lyu J, Jho E-H, Lu W (2011) Smek promotes histone deacetylation to suppress transcription of Wnt target gene brachyury in pluripotent embryonic stem cells. *Cell Res* 21:911–921.
23. Ghanem N, et al. (2007) Distinct cis-regulatory elements from the Dlx1/Dlx2 locus mark different progenitor cell populations in the ganglionic eminences and different subtypes of adult cortical interneurons. *J Neurosci* 27:5012–5022.
24. Bray SJ (2006) Notch signalling: A simple pathway becomes complex. *Nat Rev Mol Cell Biol* 7:678–689.
25. Ossipova O, Sokol SY (2010) Cell polarity, Notch signaling and neurogenesis. *Cell Cycle* 9:1–2.
26. Wei Z, et al. (2009) Klf4 interacts directly with Oct4 and Sox2 to promote reprogramming. *Stem Cells* 27:2969–2978.
27. Wojtowicz JM, Kee N (2006) BrdU assay for neurogenesis in rodents. *Nat Protoc* 1: 1399–1405.
28. Koh SS, et al. (2002) Synergistic coactivator function by coactivator-associated arginine methyltransferase (CARM) 1 and beta-catenin with two different classes of DNA-binding transcriptional activators. *J Biol Chem* 277:26031–26035.
29. Boyer LA, et al. (2005) Core transcriptional regulatory circuitry in human embryonic stem cells. *Cell* 122:947–956.
30. Bajpai R, et al. (2010) CHD7 cooperates with PBAF to control multipotent neural crest formation. *Nature* 463:958–962.